Inflammation, Vol. 47, No. 4, August 2024 (© 2024)
https://doi.org/10.1007/s10753-023-01965-5

RESEARCH

Auraptene Mitigates Colitis Induced by Dextran Sulfate Sodium in Mice by Regulating Specific Intestinal Flora and Repairing the Intestinal Barrier

Tong Chen[1] , Naizhong Jin[1] , Qi Zhang[1] , Zhongming Li[1] , Qiutao Wang[1] and Xuedong Fang[1,2]

Received 14 October 2023; accepted 29 December 2023

Abstract—Auraptene (AUT) is widely known to possess both antioxidant and anti-inflammatory properties. This study attempted to evaluate the protective effects of AUT in dextran sodium sulfate (DSS)-induced colitis in mice and to determine the underlying molecular mechanisms. Our results suggest that AUT substantially minimizes the severity and worsening of DSS-induced colitis in mice, indicated by the lengthening of the colon, lower disease activity index, reduced oxidation levels, and attenuated inflammatory factors. Molecular studies revealed that AUT reduces the nuclear translocation of nuclear factor-κB (NF-κB), thereby inhibiting the expression of inflammatory factors. Additionally, AUT promotes the diversity of the intestinal flora in mice with colitis by increasing the number of beneficial bacteria such as *Lactobacillaceae* and lowering the number of harmful bacteria. In conclusion, AUT mitigates DSS-induced colitis by maintaining the integrity of the intestinal barrier and modulating the levels of the intestinal microbial species.

KEY WORDS: Auraptene; intestinal barrier; *Lactobacillaceae*; NF-κB

INTRODUCTION

Inflammatory bowel disease (IBD), a recurrent inflammatory disease that affects the bowels, has a high incidence in developed countries and a rising occurrence in developing countries [1]. Although the specific cause of ulcerative colitis (UC) is unknown, various factors including genetic susceptibility, dysregulation of immune responses, impaired intestinal barrier, and intestinal flora imbalance have been found to contribute to the development and progression of UC [2, 3]. Currently, the primary treatment for UC involves glucocorticoid hormone administration, which has some major side effects such as edema, glucose metabolism disorder, and electrolyte imbalance [4].

A functional intestinal epithelial barrier is essential for intestinal homeostasis as it resists intestinal invasion by harmful substances and induces immune responses to pathogens, thereby protecting the host [5]. Studies have shown that UC disrupts the intestinal barrier, enabling pathogens and antigens to cross the barrier, leading to an exacerbation in the inflammatory

[1]Department of Gastrointestinal Colorectal Surgery, China-Japan Union Hospital of Jilin University, Changchun 130033, China
[2]To whom correspondence should be addressed at Department of Gastrointestinal Colorectal Surgery, China-Japan Union Hospital of Jilin University, Changchun, 130033, China; fangxd@jlu.edu.cn

responses and compromise on the barrier integrity [6]. Significant dysregulation of the tight junction proteins, including the claudin family, zonula occludens-1 (ZO-1), and occludin, has been observed in patients with IBD. Therefore, the maintenance of the expression of the tight junction proteins plays a central role in both protecting the structural integrity of the intestinal barrier and regulating its permeability and, thus, is an important target for the therapeutic management of UC [7–9].

The gut is a complex anaerobic environment consisting of a large number of microorganisms, which help maintain the intestinal barrier function, regulate the immune response, and prevent the proliferation of intestinal pathogens [10]. A balanced gut microbiota establishes a beneficial symbiotic relationship with the host [11]. Studies have shown that the disruption of the intestinal barrier and abnormal immune responses in patients with UC disrupt the host-microbe symbiosis, resulting in a reduction in the number of beneficial bacteria and an increase in the number of pathogenic bacteria in the intestine [12]. Conversely, this imbalance in the intestinal flora can also greatly increase the susceptibility to UC [13]. Therefore, therapeutic strategies promoting the maintenance of the gut microbial balance are a potential treatment option for patients with UC.

Auraptene (AUT) is a natural compound widely found in several citrus fruits such as oranges, lemons, and grapefruits [14]. Previous studies have shown that AUT is a potential drug for a variety of diseases owing to its various biological properties, including anti-cancer, anti-inflammatory, and immunomodulatory activities, and its protective effect against diseases such as metabolic disorders of the gastrointestinal organs [15]. However, the effect of AUT treatment in UC models has not been reported previously. Therefore, this study utilized a DSS-induced UC mouse model to investigate the impact of AUT treatment on UC and to determine its underlying mechanisms of action.

MATERIALS AND METHODS

Material

Aurapten and DSS were supplied by Shanghai YuanYe Biotechnology Co., Ltd. (Shanghai, China) and MP Biomedicals (Santa Ana, CA), respectively.

Animal Experiments

Thirty-six male C57BL/6 J mice aged 6–8 weeks (SPF grade) weighing 20 ± 2 g were purchased from Liaoning Changsheng Technology (Liaoning, China). The mice were housed in a certified standard laboratory cage at a temperature of 23–26 ℃. All the mice were provided food and water with no restrictions. After the mice were well adapted to the environment (about a week), they were randomly divided into 6 groups, namely control (no treatment), DSS (2.5%), AUT (80 mg/kg), and DSS+AUT (20, 40, and 80 mg/kg) groups, with $n = 6$ mice in every group. The mice in the AUT and DSS+AUT groups (20, 40, and 80 mg/kg) were administered AUT for 14 days during the course of the experiment. On days 18–25, DSS (2% w/v) was added to the drinking water supplied to all the groups except the control and AUT groups to construct a colitis mouse model (Fig. 1a). The weight, diet, and stool status of the mice were recorded daily. The mice were anesthetized and euthanized on day 25. Subsequently, the colon tissues were collected, and some of the colon tissue was stored in 4% formaldehyde, and the remaining tissue was stored at − 80 ℃. Fecal samples were also collected from the mice and stored at − 80 ℃.

Cell Culture and Treatment

Human epithelial cell line Caco-2 was obtained from the Chinese Academy of Sciences (Shanghai, China) Cell Bank. Caco-2 cells were cultured in high-glucose DMEM supplemented with 10% fetal bovine serum, 100 U/mL penicillin, and 100 U/mL streptomycin. The cells were cultured in 5% CO_2 in an incubator at 37 ℃. The cells were then treated with AUT (20 μM, 50 μM, and 100 μM) for 24 h and incubated with LPS (1 μg/mL) for 2 h. Subsequently, the expression of the intestinal barrier proteins was detected by Western blot analysis.

CCK-8 Assay

Caco2 was inoculated into 96-well plates, treated with AUT at concentrations of 0 μM, 5 μM, 10 μM, 20 μM, 50 μM, 100 μM, and 200 μM for 24 h, then added with 10 μL CCK-8 solution for 2 h, and absorbance was determined at 450 nm.

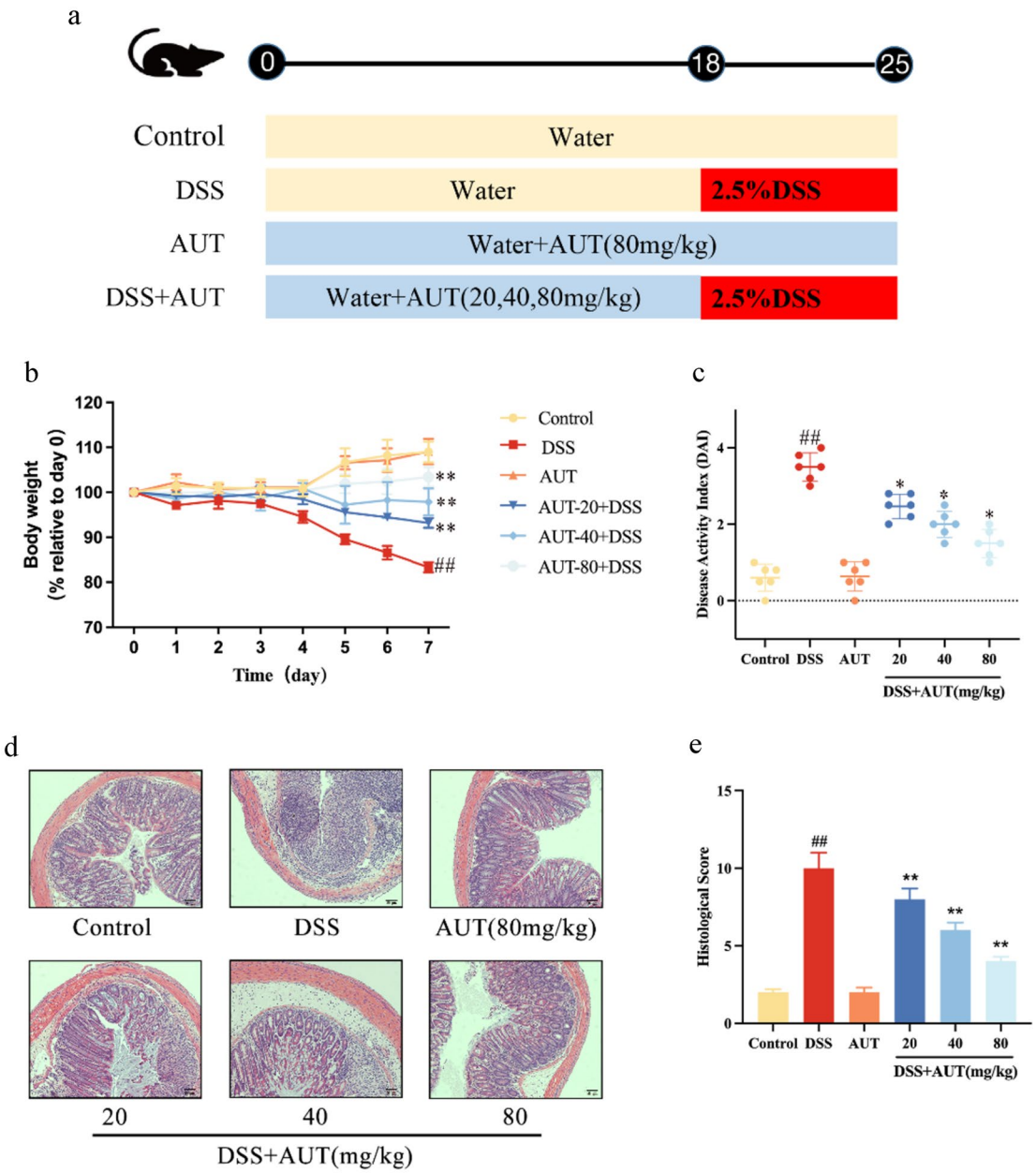

Fig. 1 Auraptene (AUT) alleviates colitis symptoms and colon damage caused by DSS in mice. **a** Schematic diagram of the experimental design. **b** Weight change in mice in every group. **c** Disease activity index (DAI) changes in every group. **d** H&E staining of the colon tissue samples from mice in every group. The magnification is 100x. **e** Colonic histopathological score. All data are represented as mean ± SEM ($n = 6$). #$p < 0.05$ and ##$p < 0.01$ vs. control group; *$p < 0.05$ and **$p < 0.01$ vs. DSS group.

Disease Activity Index (DAI)

The weight changes, rectal bleeding (hematochezia), and fecal status were recorded daily during DSS treatment. The specific scoring rules followed are listed below: weight (0 point, 0%; 1 point, 1–5%; 2 points, 5–10%; 3 points, 10–15%; and 4 points, 15%); consistency of the stool (0 point: normal; 1–3 points: loose; 4 points: diarrhea); and rectal bleeding (0 point: negative; 1–3 points: positive; and 4 points: gross bleeding).

Hematoxylin and Eosin (H&E) Staining

After collecting the colon, the distal colon tissue was fixed in 4% formaldehyde for 24 h, transferred to alcohol for dehydration, and subjected to paraffin embedding. The colon tissue samples were then cut into 3–5-μm sections using a microtome and subjected to H&E staining to identify any histopathological alterations, which were detected by observation under an optical microscope.

Colon Histological Score

Three H&E-stained sections of the colon were randomly selected and scored by three pathology experts. The scoring criteria mainly refer to previous descriptions [16], as shown in Table 1.

Immunofluorescence Staining

The colon tissue sections were dewaxed using xylene and dehydrated by exposure to an ethanol gradient. Thereafter, they were sealed by placing them in 0.1% Triton X-100 solution diluted with PBS. They were then placed in 95% citrate buffer for antigen repair, washed thrice with PBS with each wash lasting five minutes, and sealed with 5% donkey serum for one hour. A 5% donkey serum (1:200) was also used to dilute the primary antibody. The colon tissues were incubated with the primary antibody overnight at 4 °C. After washing thrice with PBS with each wash lasting 5 min, the tissues were incubated with a secondary antibody diluted with a 5% donkey serum (1:1000) for 1 h, washed thrice with PBS for 5 min each time, dyed with DAPI, and observed under an optical microscope.

Permeability of the Intestinal

The fluorescein isothiocyanate (FITC)-Dextran 4000 (4 kDa, Cat# FD4, Sigma, MO, USA) test was used to measure intestinal permeability. Mice were given FITC-dextran 4000 (600 mg/kg) by gavage after they had been fasted for 4 h. Whole blood was collected, and serum was separated 4 h after gavage. Using a multimode plate reader (PerkinElmer EnSpire Plate Reader, Waltham, USA) (excitation, 490 nm; emission, 520 nm), the fluorescence intensity of FITC-dextran 4000 in plasm was analyzed. By dilution in PBS, standard curves for FITC-dextran concentration calculations were generated.

Detection of Myeloperoxidase (MPO) Activity

One part of the colon tissue obtained was completely ground with N-2-hydroxyethyl piperazine-N-ethane-sulfonic acid (HEPES) and centrifuged at 4 ℃ at 12000 rpm for 10 min. The supernatant was collected and subjected to enzyme-linked immunosorbent assay (ELISA). The precipitate was further ground with 0.5% cetyltrimethylammonium chloride (CTAC) and centrifuged at 12,000 rpm at 4 ℃ for 10 min. Subsequently, the supernatant was collected and added to a 96-well plate along with the substrate resulting in a reaction. After 3 min, sulfuric acid was added to the plate to stop the reaction. The absorbance was measured at 450 nm.

ELISA and Oxidative Stress Markers Analysis

The colon tissue was ground with HEPES, and the supernatant was collected. The expression levels of IL-1β, TNF-α, and IL-6 in the colon tissues of mice were measured using an ELISA kit (Beijing Solarbio Science & Technology Co., Ltd.). All ELISA kits were

Table 1 The standard scoring system of disease activity index (DAI)

Score	Body weight loss	Feces status	Bloody stools
0	No loss	Normal	No blood (no color within 2 min)
1	1 ~ 5%	Loose stool (not attached to the anus)	Presence (within 1–2 min, fuchsia)
2	5% ~ 10%	Loose stool (attach to the anus)	Presence (within 1 min, fuchsia)
3	10% ~ 15%	Diarrhea (liquid)	Presence (within 10 s, purplish blue)
4	> 15%	Severe diarrhea	Gross blood (instantly purplish blue)

purchased from Wuhan Servicebio Biological Engineering Co. Ltd. (Wuhan, China). The levels of certain oxidative stress markers (superoxidase dismutase (SOD), catalase (CAT), reduced glutathione (GSH), and malondialdehyde (MDA)) were measured according to the manufacturer's instructions.

Western Blotting

A suitable amount of NP40 lysate (Biyuntian, Wuhan, China) was added to the colon tissue. The tissue was completely ground and centrifuged at 12,000 rpm for 10 min, and the supernatant was collected. The BCA protein assay kit (Thermo Scientific, China) was employed, and the protein concentration was determined. The samples were divided into the same concentration and separated on a 12% gel using sodium dodecyl sulfate–polyacrylamide gel electrophoresis (SDS-PAGE). The isolated protein was transferred to a polyvinylidene difluoride (PVDF) membrane. Next, they were closed at room temperature (RT) for 3 h, and the film was incubated at 4 ℃ overnight with the primary antibody. The membrane was washed with TBS-T four times (15 min each time) and incubated with the enzyme-labeled secondary antibody at RT for 1 h. The membrane was again washed with TBS-T 4 times (15 min each time). After the development of the protein bands, the bands were observed using a chemiluminescent reagent (Beyotime, Shanghai, China). ImageJ as well as GraphPad Prism software was used to analyze the protein expression levels. The antibodies used in this study are listed below: anti-iNOS (ProteinTech, Wuhan, China), anti-COX-2 (ProteinTech, Wuhan, China), anti-Claudin3 (Abcam, Shanghai, China), anti-INOS (Proteintech, Wuhan, China), anti-COX-2 (Proteintech, Wuhan, China), anti-ZO-1 (ProteinTech, Wuhan, China), anti-TLR4 (Cell Signaling Technology, Danvers, MA), anti-p-NF-κB P65 (Cell Signaling Technology, Danvers, MA), anti-NF-κB P65 (Cell Signaling Technology, Danvers, MA), anti-p-IκB (Cell Signaling Technology, Danvers, MA), anti-p-IκB (Cell Signaling Technology, Danvers, MA), anti-β-actin (Santa, Shanghai, China), goat anti-mouse IgG (BOSTER, Wuhan, China), and goat anti-rabbit IgG (BOSTER, Wuhan, China).

16SrRNA and Short-Chain Fatty Acid Sequencing

The feces of mice were collected on the day before dissection, and the fecal DNA was extracted using the DNA rapid extraction kit according to the manufacturer's instructions. Fecal DNA samples were shipped to Shanghai Pacenol Technology Co., Ltd., and PCR was performed on the V3-V4 hypervariable region of 16S rRNA. After Qubit quantification of DNA concentration and qualified library detection, the constructed library was sequenced on an Illumina IonS5TM XL platform.

A total of 100 mg of fresh cecal contents were accurately weighed into a 2 mL grinding tube, and grinding beads and 1 mL of water containing 0.5% phosphoric acid and 50 μg/mL internal standard 2-ethylbutyric acid were added to the tube. The cecal contents were ground twice at 50 HZ for 3 min in a frozen grinding machine, placed in an ice water bath, and subjected to ultrasound treatment for 30 min. Subsequently, the contents were allowed to stand at 4 ℃ for 30 min and centrifuged at 4 ℃ at 13,000 g for 15 min. The supernatant was collected in a new 1.5 mL centrifuge tube, and 500 μL of ethyl acetate was added to the supernatant for extraction. The solution was mixed by vortexing, placed in an ice water bath for 10 min, and centrifuged at 4 ℃ at 13,000 g for 10 min. Subsequently, the supernatant solution was taken on the machine for analysis.

Statistical Analysis

Each experiment was repeated independently at least thrice. Graphs were drawn using GraphPad Prism 9.0. The differences between relevant groups of data were analyzed using SPSS 21.0. One-way ANOVA was used to analyze the differences between three or more sets of data. $P < 0.05$ and $P < 0.01$ were used to indicate a statistically significant difference.

RESULTS

AUT Alleviates DSS-Induced Colitis Symptoms and Colon Damage in Mice

This mouse model was used to evaluate whether AUT alleviates the severity of colitis (Fig. 1a). During the modeling period, weight measurement and DAI scoring were performed daily. The results showed that contrary to the control group, DSS treatment led to a significant decrease in the body weight and an increase in the DAI score, while the administration of AUT alleviated the loss in body weight and restored the DAI score

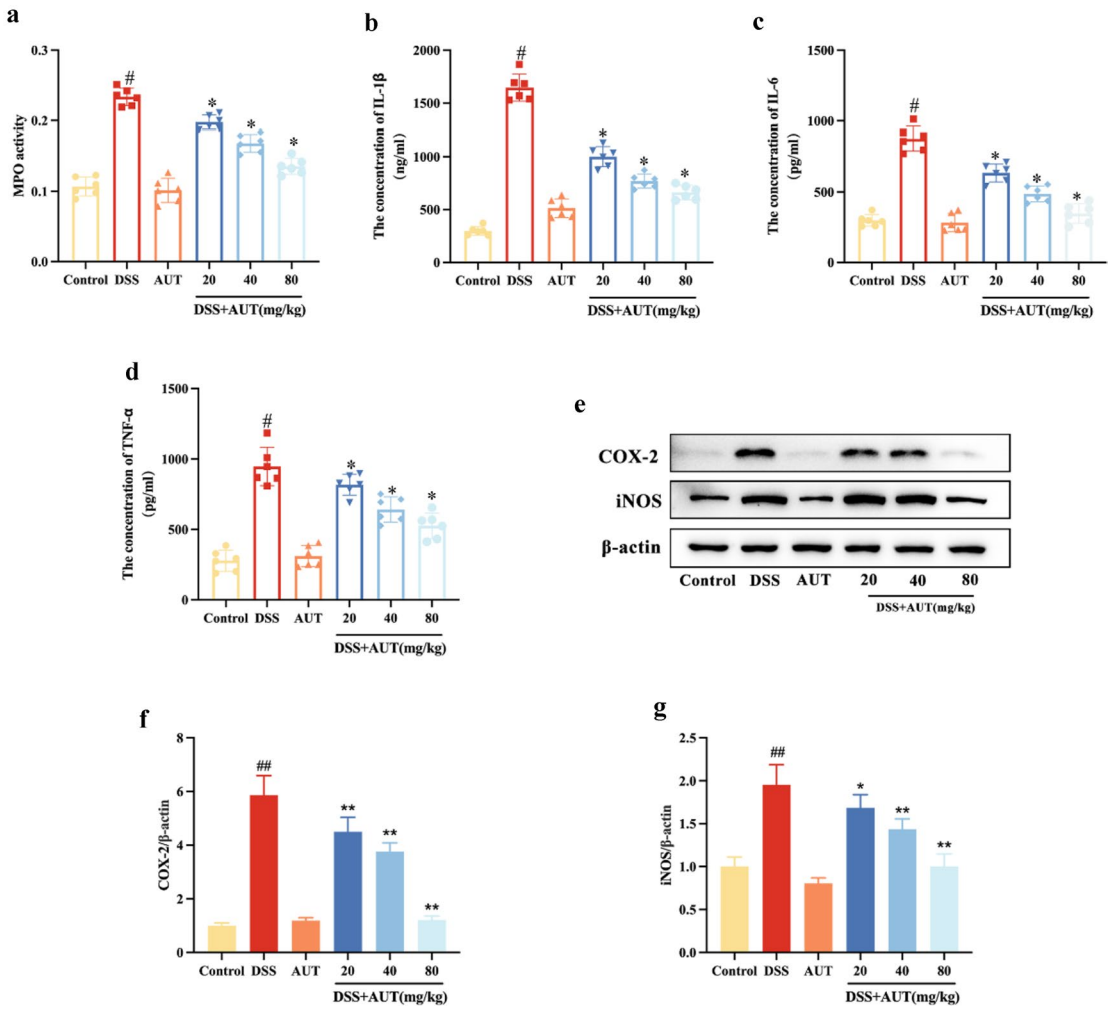

Fig. 2 Alleviation of DSS-induced colon inflammation by AUT in mice. **a** MPO activity of colon tissue from mice in each group. **b–d** Levels of IL-1β, TNF-α, and IL-6 proteins in the colon tissue of mice as detected by ELISA. **e–g** Protein levels of COX-2 and iNOS in the colon tissue of mice as detected by Western blotting. β-Actin is the internal control. All data are shown as mean ± SEM ($n = 6$). #$p < 0.05$ and ##$p < 0.01$ vs. control group; *$p < 0.05$ and **$p < 0.01$ vs. DSS group.

in a dose-dependent manner (Fig. 1b, c). To evaluate the colonic injury, we studied the histopathological changes in the colon using H&E staining. The findings affirmed that DSS treatment caused colonic crypt destruction, submucosal edema, and accumulation of inflammatory cells in mice. Additionally, the histopathological score was also significantly higher than that in the Control group. Conversely, AUT mitigated these pathological lesions in a dose-dependent manner (Fig. 1d, e). Collectively, these data suggest that the administration of AUT before DSS treatment alleviates DSS-induced colitis symptoms and colon damage in mice.

AUT Alleviates DSS Induced Colon Inflammation in Mice

To further explore the impact of AUT on DSS-induced colitis in mice, we evaluated the anti-inflammatory impacts of AUT. First, MPO activity was detected to determine the degree of moistening of the neutrophils in the colon tissue. The findings revealed that the MPO activity of mice in the DSS group was significantly higher than that in the control group. However, AUT administration led to an improvement in the MPO activity (Fig. 2a). Subsequently, the levels of certain pro-inflammatory

cytokines (IL-1β, IL-6, and TNF-α) and pro-inflammatory enzymes (cyclooxygenase-2 (COX-2), inducible nitric oxide synthase (iNOS)) were determined. The findings affirmed that DSS treatment caused a significant elevation in the levels of pro-inflammatory factors while AUT attenuated the expression of IL-1β, TNF-α, and IL-6 in a dose-dependent manner (Fig. 2b–d). Western blot analysis revealed that AUT reduced the elevation in the protein levels of COX-2 (Fig. 2e, f) and iNOS (Fig. 2e, g), which were induced by DSS. Conclusively, these data show that AUT relieves DSS-induced colon inflammation in mice.

AUT Improves Intestinal Barrier Integrity in Mice with DSS-Induced Colitis

Disruption of intestinal barrier integrity is a major pathological feature of UC. Thus, we studied the impact of AUT on intestinal TJ protein expression. Immunofluorescence staining results revealed that the expression of claudin3 (Fig. 3a) and ZO-1 (Fig. 3a) proteins was significantly lower in the DSS group compared to the control group and that the distribution of these proteins in the colon tissue was uneven in the DSS group. However, treatment with AUT mitigated the decrease in the expression of these TJ proteins in a dose-dependent manner (Fig. 3a). Western blot analysis showed that AUT improved the decline in the expression levels of claudin-3, ZO-1, and occludin (Fig. 3b–e). FITC results also showed that intestinal barrier damage was severe in the DSS group, while the barrier was restored after AUT pretreatment (Fig. 3f). In addition, I also obtained the same results in the cell experiment (Fig. S1). These results demonstrate that AUT reduces the DSS-induced intestinal barrier damage in mice by increasing the expression levels of the TJ proteins.

AUT Inhibits TLR4/NF-κB Activation in Mice with DSS-Induced Colitis

To investigate the protective mechanism of AUT in mice with DSS-induced colitis, we examined the expression levels of several key proteins in the TLR4/NF-κB inflammation-related signaling pathway. Western blot analysis revealed that DSS significantly increased the expression level of TLR4 by activating the TLR4/NF-κB pathway, while AUT reduced the protein expression of TLR4 in a dose-dependent manner (Fig. 4a, b). Moreover, the phosphorylation levels of NF-κB p65 and IκBα proteins in the NF-κB signaling pathway revealed that AUT significantly lowered the levels of key proteins in the NF-κB pathway (Fig. 4a, c, d). These data suggest that the protective effect of AUT on DSS-induced colon inflammation in mice is closely linked to the inhibition of the activation of the TLR4/NF-κB signaling pathway.

AUT Inhibits Oxidative Stress in Mice with DSS-Induced Colitis

As seen in Fig. 5, DSS significantly decreased the activities of SOD, GSH, and CAT, while significantly increasing the activity of MDA. Conversely, AUT treatment reversed this effect and led to a significant increase in the activities of SOD (Fig. 5a), GSH (Fig. 5b), and CAT (Fig. 5c), while significantly decreasing the activity of MDA (Fig. 5d). These results demonstrate that AUT intervention alleviates oxidative stress in colon tissue.

AUT Enhances the Levels of Short-Chain Fatty Acids in Mice with DSS-Induced Colitis

As seen in Fig. 6, DSS treatment led to a significant reduction in the levels of acetic acid, propionic acid, butyric acid, and valerate, while AUT prophylaxis led to a significant increase in the levels of acetic acid (Fig. 6a), propionic acid (Fig. 6b), butyric acid (Fig. 6c), and valerate (Fig. 6d). These results prove that AUT intervention improves the levels of short-chain fatty acids (SCFAs) in the intestine, thus playing a role in protecting the intestine.

AUT Regulates the Diversity and Abundance of the Gut Microbiota in Mice with DSS-Induced Colitis

First, to ascertain whether AUT could alter the gut microbiota, we performed 16S rRNA sequencing. Venn diagram of the sequencing data showed that the control, DSS, and AUT-DSS groups had 4474, 1060, and 2245 distinct OTUs (Fig. 7a). PCoA analysis showed a difference in the gut microbiota between the DSS and control groups. AUT pre-conditioning improved the changes in the gut microbiota of the mice in the DSS group (Fig. 7b). The α-diversity results revealed that the Chao1 (Fig. 7c) and Shannon (Fig. 7d) indices were significantly reduced in the DSS group compared to that in the control group, indicating a reduction in flora richness.

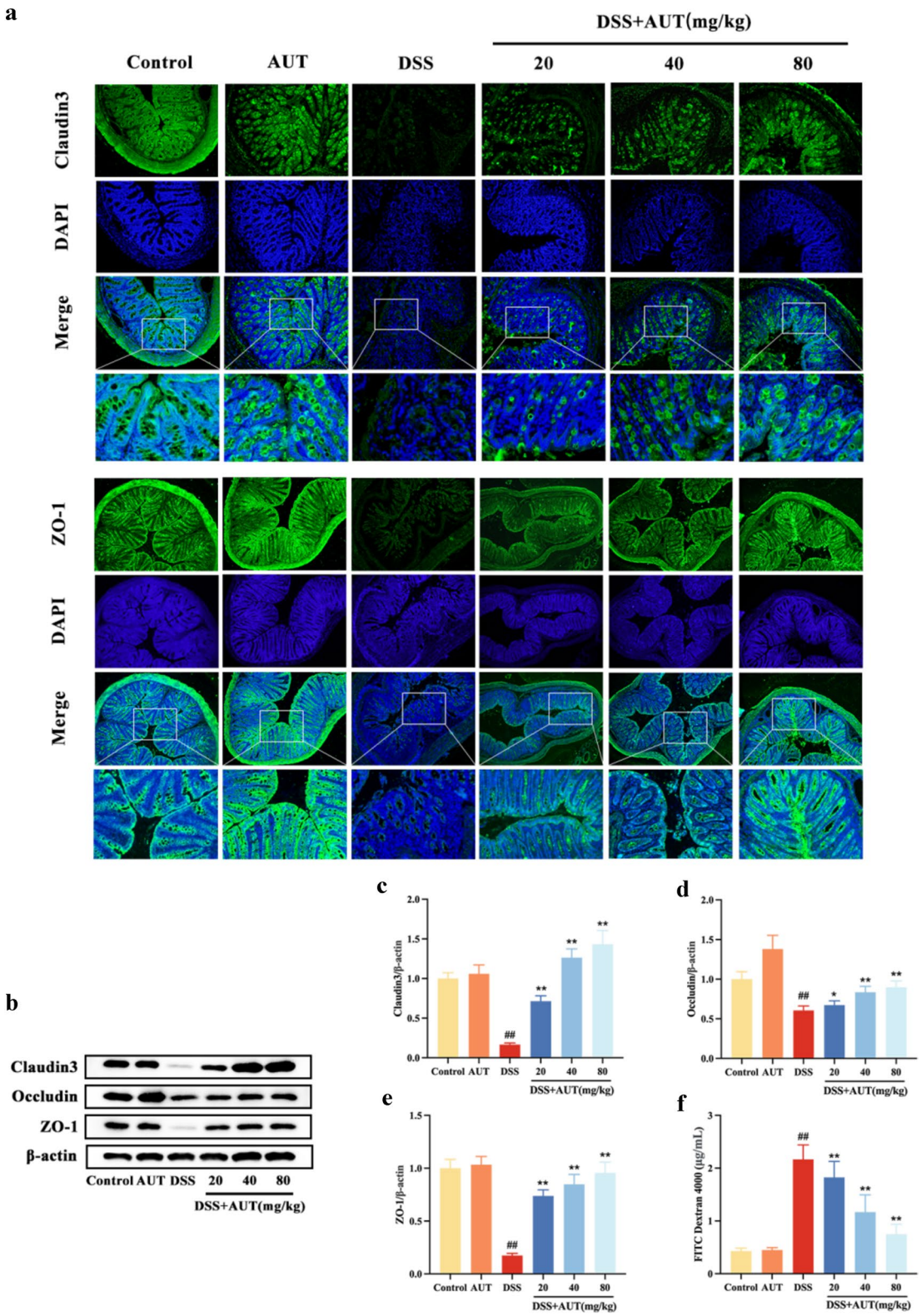
a
DSS+AUT(mg/kg)
Control
AUT
DSS
20
40
80
Claudin3
DAPI
Merge
ZO-1
DAPI
Merge
b
Claudin3
Occludin
ZO-1
β-actin
Control AUT DSS 20 40 80
DSS+AUT(mg/kg)
c
Claudin3/β-actin
d
Occludin/β-actin
e
ZO-1/β-actin
f
FITC Dextran 4000 (μg/mL)
Control AUT DSS 20 40 80
DSS+AUT(mg/kg)

◂**Fig. 3** AUT improves the integrity of the intestinal barrier for DSS-induced colitis in mice. **a** Representative immunofluorescence images of claudin3 and ZO-1 in colon tissue. The scale is 50 μm. **b**–**e** Protein levels of occludin, claudin3, and ZO-1 as detected by Western blotting of the colon tissue. β-Actin is the internal control. **f** Intestinal permeability analysis was performed by FITC Dextran 4000. All data are shown as mean ± SEM ($n = 6$). $^{\#}p < 0.05$ and $^{\#\#}p < 0.01$ vs. control group; $^{*}p < 0.05$ and $^{**}p < 0.01$ vs. DSS group.

However, the bacterial richness index increased significantly in mice pre-treated with AUT.

Figure 8a, b shows the relative abundance of the intestinal flora in mice in the different treatment groups at the phylum and genus levels, respectively. In comparison to the control group, the abundance of *Firmicutes* was significantly reduced (Fig. 8c) while the abundance of *Bacteroidetes* was significantly increased in the DSS group (Fig. 8d). Additionally, compared to the control group, the abundance of *Lactobacillaceae* (Fig. 8f), *Allobaculum* (Fig. 6g), and *Oscillospira* (Fig. 8h) was also significantly reduced in the DSS group. However, pre-treatment with AUT led to the recovery of the bacterial abundance.

Spearman analysis demonstrated that *Bacteroidetes* showed a significant negative correlation with both colon length and the intestinal barrier protein and a significant positive correlation with inflammatory factors and DAI (Fig. 9a). Conversely, *Lactobacillaceae*, *Allobaculum*, and *Oscillospira* correlated positively with colon length and intestinal barrier and negatively with inflammatory factors and DAI (Fig. 9a). Therefore, the protective effect of AUT on DSS-induced colitis may be linked to its regulation of intestinal flora.

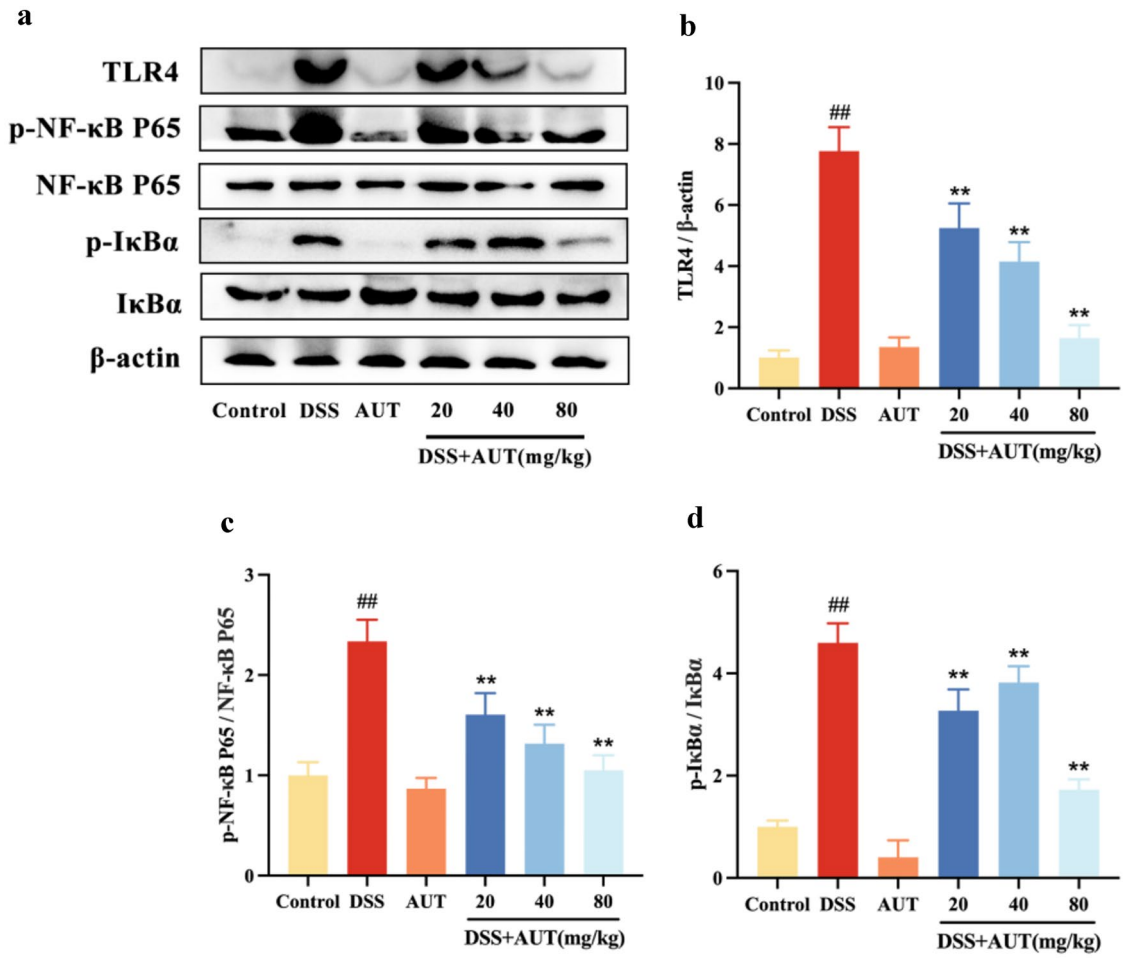

Fig. 4 AUT inhibits TLR4/NF-κB activation in mice with DSS-induced colitis. **a**–**d** Western blot analysis of TLR4 protein expression, protein phosphorylation, NF-κB p65, and IκB in the colon tissue of mice in each group. β-Actin is the internal control. All data are shown as mean ± SEM ($n = 6$). $\#p < 0.05$ and $\#\#p < 0.01$ vs. control group; $*p < 0.05$ and $**p < 0.01$ vs. DSS group.

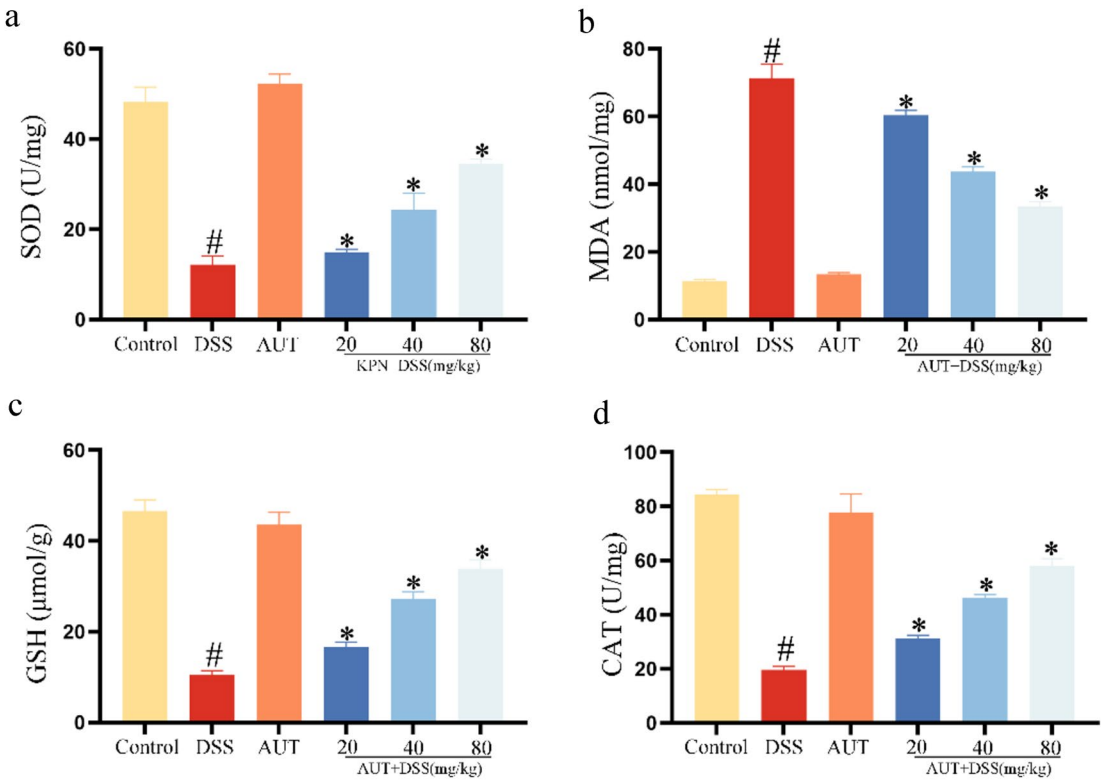

Fig. 5 AUT inhibits oxidative stress in mice with DSS-induced colitis. (A) Activity of SOD (**a**), MDA (**b**), GSH (**c**), and CAT (**d**) in the colon tissue of mice as detected by kit method. All data are shown as mean ± SEM ($n = 6$). #$p < 0.05$ vs. control group; *$p < 0.05$ vs. DSS group.

DISCUSSION

AUT, an umbelliferone coumarin, is widely distributed in certain edible fruits and vegetables, such as oranges, lemons, and grapefruits [17]. A previous study has reported that AUT has anti-diabetic, anti-inflammatory, anti-cancer, and antibacterial pharmacological activities [18]. However, its protective effect against UC and the underlying mechanisms of action are unclear. Thus, we ascertained the regulatory effect of AUT on a DSS-induced colitis mouse model. We found that AUT reduced body weight loss and colon tissue injury, lowered the expression levels of the pro-inflammatory mediators, reversed the reduced expression of the TJ proteins, and protected intestinal barrier integrity during UC. A previous study has shown that AUT can ameliorate intestinal flora imbalance and inhibit the activation of the TLR4/NF-κB signaling pathway. These studies demonstrate that AUT improves DSS-induced colitis in mice by inhibiting inflammatory responses, modulating intestinal flora, and maintaining intestinal barrier integrity.

Weight loss, DAI, and colon tissue scores are often used as primary parameters to determine the severity of UC. The clinical features of DSS-induced colitis in mice are similar to those in patients with UC [19, 20]. In our study, the administration of AUT significantly improved weight loss, reversed the elevation in DAI that led to the destruction of crypts in colon tissue, and purged the inflammatory cells.

During UC, the colon tissues contain a large number of neutrophils, and MPO, a heme-containing peroxidase, is highly expressed in the inflammatory cells, which in this case are predominantly neutrophils [21]. Moreover, during UC, the neutrophils and macrophages secrete pro-inflammatory mediators like TNF-α, IL-1β, iNOS, COX-2, and IL-6 in large quantities, which are the most important factors responsible for intestinal mucosal inflammation [22]. In this study, we found that DSS

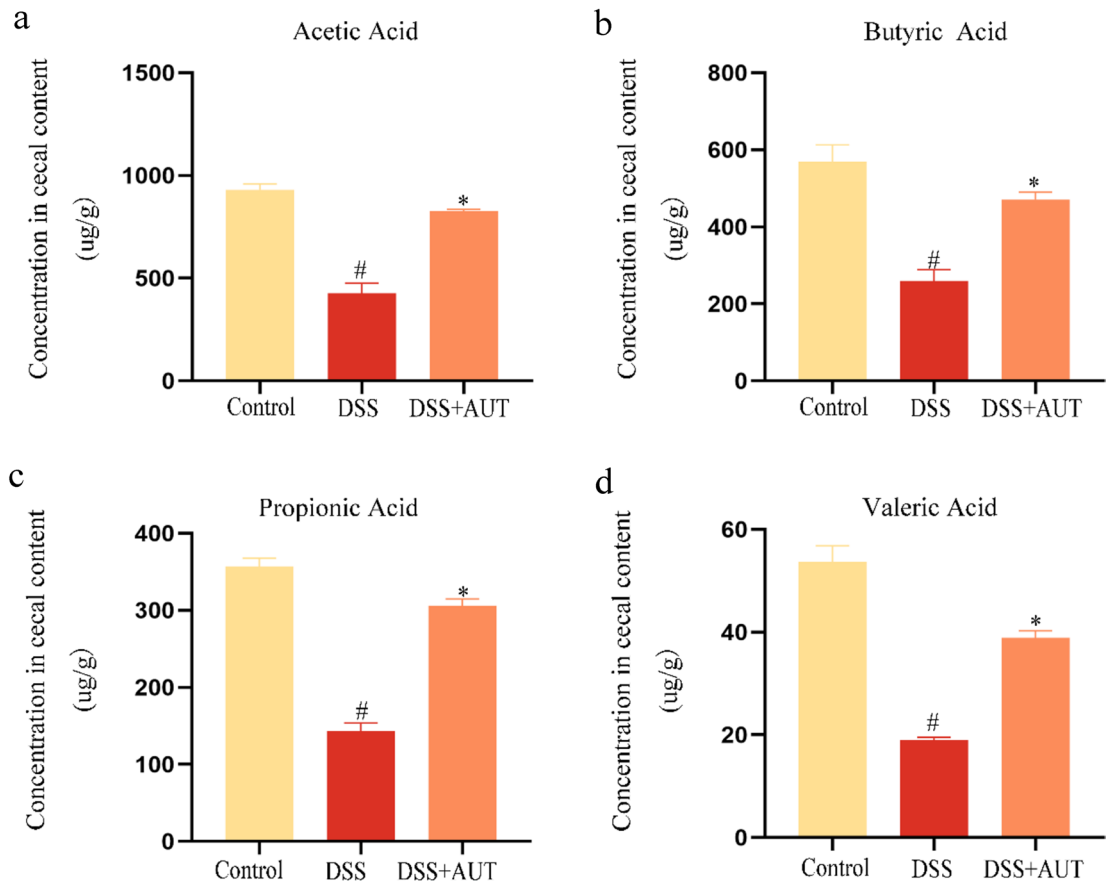

Fig. 6 AUT increases the levels of short-chain fatty acids in mice with DSS-induced colitis. **a** Acetic acid content. **b** Butyric acid content. **c** Propionic acid content. **d** Valeric acid content. All data are shown as mean ± SEM ($n = 6$). #$p < 0.05$ vs. control group; *$p < 0.05$ vs. DSS group.

treatment significantly increased the MPO activity in the colon tissue of mice and aggravated colon tissue injury. Interestingly, AUT not only reduced MPO activity, but also inhibited the excessive secretion of pro-inflammatory mediators and alleviated DSS-induced colon inflammation in mice.

The beneficial role of SCFAs in UC has been widely reported. SCFAs maintain the intestinal mucosal chemical barrier by activating GPCRs, which upregulate the expression of mucosal proteins and antimicrobial peptides [23]. In addition, SCFAs can act on a variety of immune cells. They alter gene expression, affect the proliferation and apoptosis of immune cells, and regulate intestinal inflammation [24]. In this study, we found that AUT prophylaxis significantly increased the reduction in the levels of exercise-induced fatty acids in mice with DSS-mediated colitis.

The intestinal epithelial mucosa is vital in maintaining intestinal permeability by serving as a barrier between the internal and external environments [25]. This barrier functions through a structure called the "tight junction," which is composed of many complete membrane proteins and related cytoplasmic proteins, the most prominent of which are transmembrane barrier proteins (occludin and claudin) and cytoplasmic scaffold proteins (ZO family). Examples of tight junction proteins include occludin, claudin-3, and ZO-1 [26]. Previous studies have shown that patients with UC often exhibit a downregulation in the expression of the TJ proteins, leading to increased intestinal permeability and decreased ability to inhibit

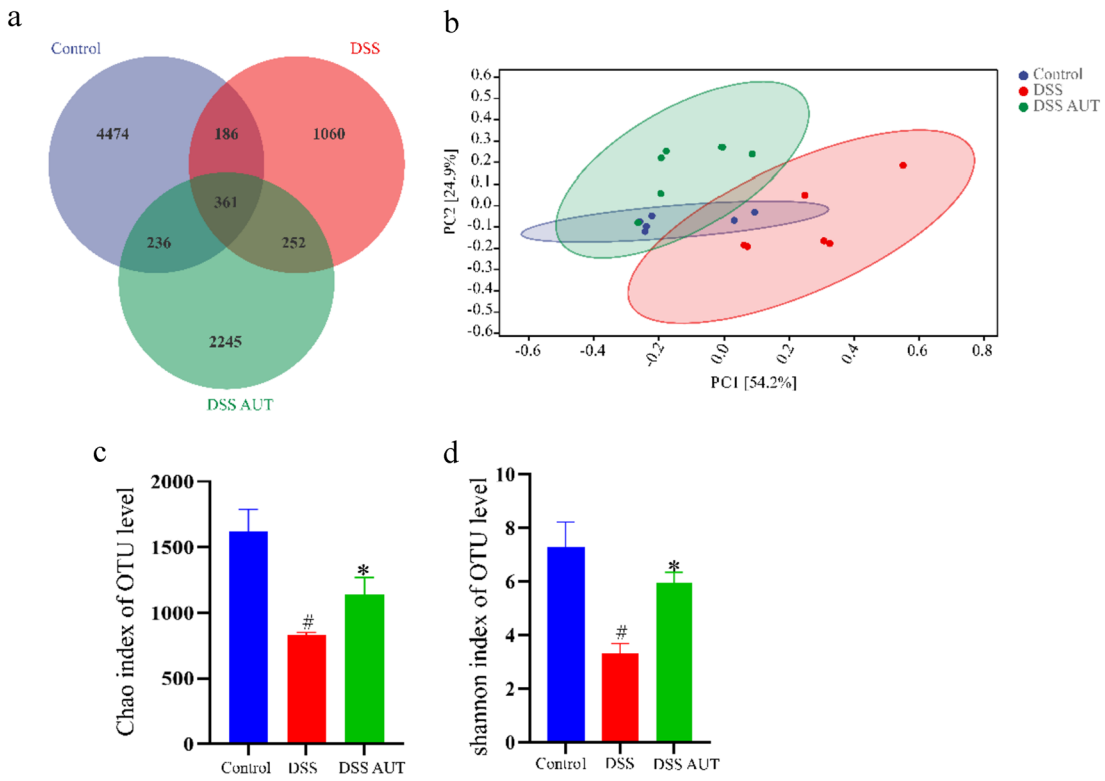

Fig. 7 Impact of AUT on the structure of the intestinal microflora in mice with DSS-induced colitis. **a** Venn diagram depicting the OTUs in the Control, DSS, and AUT (80 mg/kg)-DSS groups. **b** PCoA analysis using weighted UniFrac distance. **c** Chao index. **d** Shannon index. All data are shown as mean ± SEM ($n = 6$). #$p < 0.05$ and ##$p < 0.01$ vs. control group; *$p < 0.05$ and **$p < 0.01$ vs. DSS group.

pathogen invasion, which in turn exacerbates the inflammatory response [27]. In this study, we found that DSS treatment led to the destruction of the intestinal barrier while AUT alleviated this damage to the barrier by enhancing the expression of the TJ proteins. Similar results were achieved *in vitro* as well.

Toll-like receptors (TLR) play a crucial role in innate immunity. Activated TLRs are important for effective defense against invading pathogens [28, 29]. Multiple signaling pathways are implicated in the inflammatory response triggered by TLR4. TLR4 activation can trigger the NF-kB signaling pathway downstream, which regulates the expression of certain pro-inflammatory factors such as IL-6, IL-1β, and TNF-α [30], which in turn can enhance the activation of NF-κB [31]. Prior studies have shown that NF-κB is linked to the progression of colitis and is a key target for UC therapy. This study revealed that AUT treatment inhibits the activation of the TLR4/NF-κB signaling pathway, thereby modulating the DSS-induced inflammatory response in the colon. Extensive literature bears evidence of the anti-inflammatory effects of AUT on LPS-stimulated RAW 264.7 cells. Therefore, we speculate that AUT can also play an anti-inflammatory role *in vitro*.

Previous clinical trials have reported a reduction in the *Firmicutes*-to-*Bacteroidetes* ratio in the gastrointestinal tract microbiota of mice models with colitis [32]. A similar result was also observed in this study. However, the *Firmicutes*-to-*Bacteroidetes* ratio was effectively restored by AUT treatment. At the genus level, *Lactobacillaceae* are well-known probiotic bacteria that help reduce the risk of intestinal inflammation [33]. In this study, the results showed a significant increase in the number of *Lactobacillaceae* in the AUT treatment group compared to the DSS group. Further, we found a negative and positive correlation between *Lactobacillaceae*

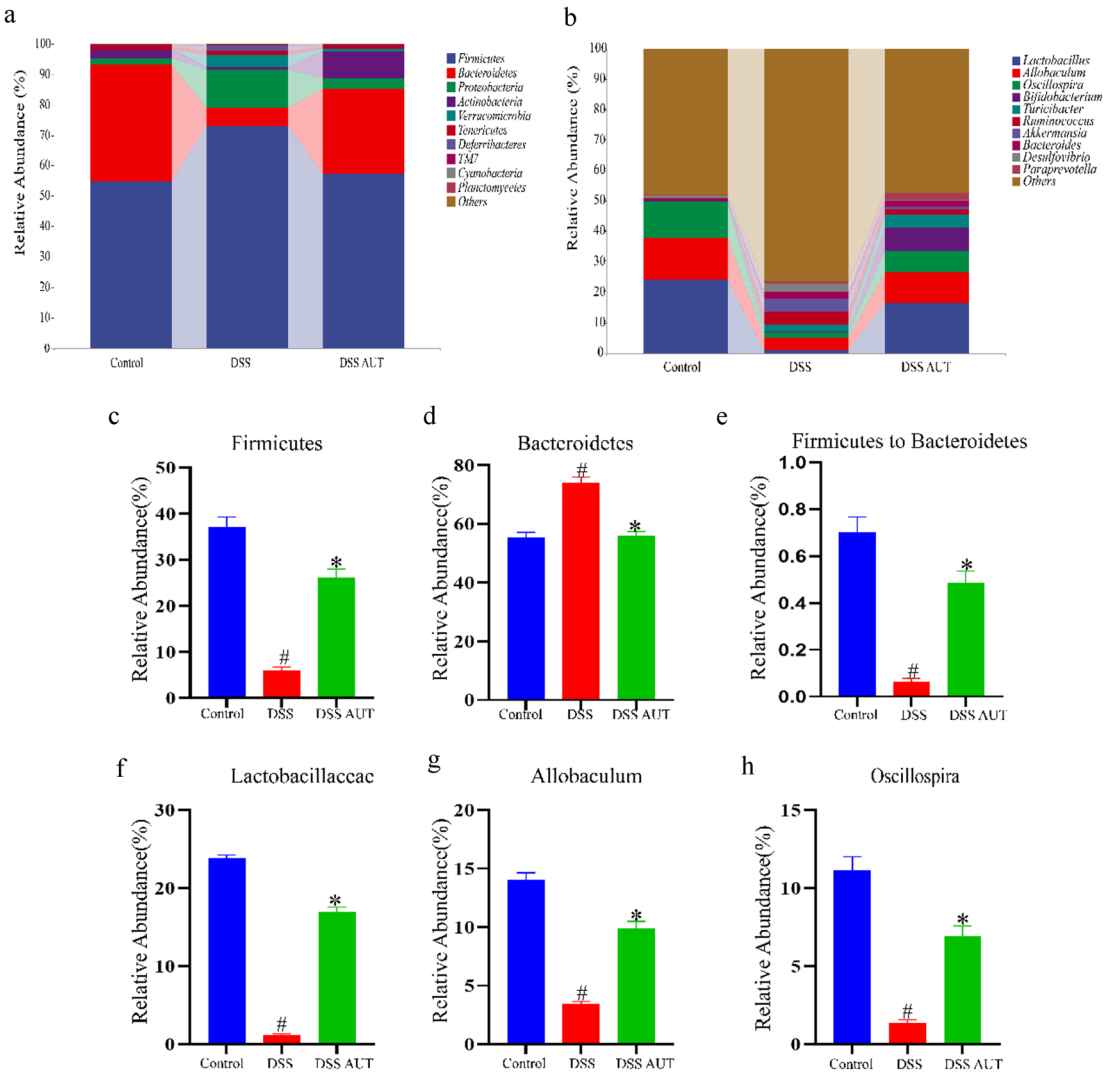

Fig. 8 Effect of AUT on specific intestinal flora in mice with DSS-induced colitis. **a**, **c**, **d**, **e** Composition of the intestinal microbiota at the phylum level. **b**, **f**, **g**, **h** Composition of the intestinal microbiota at the genus level. All data are shown as mean ± SEM ($n = 6$). #$p < 0.05$ and ##$p < 0.01$ vs. control group; *$p < 0.05$ and **$p < 0.01$ vs. DSS group.

and DAI, inflammatory factors, and colon length, respectively. Furthermore, a previous study has shown that *Allobaculum* has a protective effect on body metabolism and inflammation [34]. In this study, the results showed that AUT treatment increased the DSS-induced decrease in *Allobaculum* abundance and that *Allobaculum* was inversely associated with DAI and inflammatory factors. Previous studies have shown that *Oscillospira* produces SCFAs, which alleviate inflammatory diseases. In this study, we found that AUT can significantly increase the number of *Oscillospira* species and that the *Oscillospira* population is proportional to the intestinal barrier.

In conclusion, early intervention with AUT can significantly alleviate UC by regulating the intestinal ecological imbalance, thereby indicating that AUT can serve as a food additive in the future for alleviating the symptoms of UC.

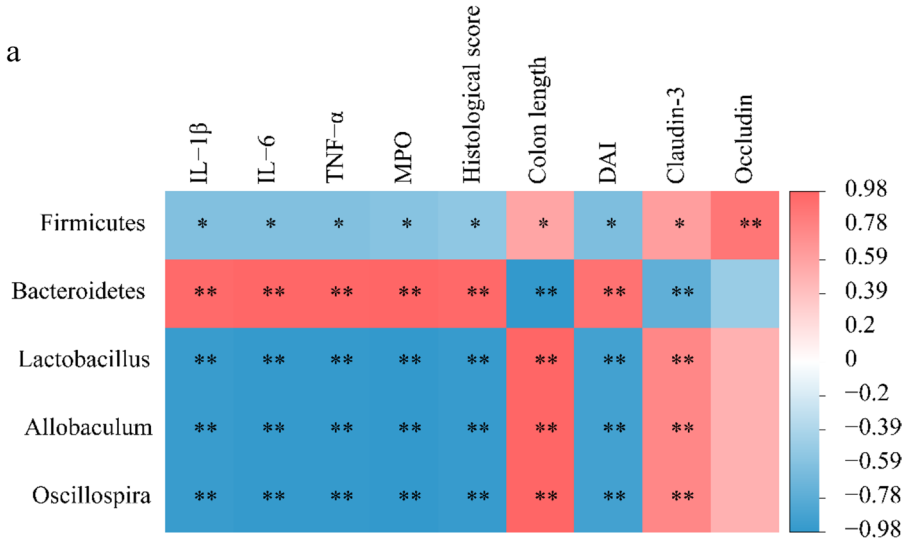

Fig. 9 Effect of AUT on dominant microorganisms. **a** Correlation analysis between intestinal barrier, colon inflammatory cytokines, colon length, and intestinal flora. The red and blue blocks denote positive and negative correlations, respectively. The color grade denotes the correlation degree. $^{*}p < 0.05$, $^{**}p < 0.01$.

SUPPLEMENTARY INFORMATION

The online version contains supplementary material available at https://doi.org/10.1007/s10753-023-01965-5.

AUTHOR CONTRIBUTION

Conceptualization: Xuedong Fang, Tong Chen, Naizhong Jin, Zhongming Li, and Qiutao Wang. Methodology: Qiutao and Tong Chen. Formal analysis: Xuedong Fang and Naizhong Jin. Investigation: Zhongming Li, Qiutao Wang, and Tong Chen. Data curation: Tong Chen. Writing—original draft: Xuedong Fang. Writing—review and editing: Qiutao Wang.

FUNDING

This study was supported by the Norman Bethune Program of Jilin University (Grant No. 2022B15) and the Science and Technology Development Program of Jilin Province (Grant Nos. YDZJ202301ZYTS103 and YDZJ202201ZYTS002).

DATA AVAILABILITY

The data supporting the findings in this study will be made available upon reasonable request to the corresponding authors.

DECLARATIONS

Conflict of interest The authors declare no competing interests.

REFERENCES

1. Wei, Y.Y., et al. 2021. Shaoyao decoction attenuates DSS-induced ulcerative colitis, macrophage and NLRP3 inflammasome activation through the MKP1/NF-κB pathway. *Phytomedicine* 92: 153743.
2. Xu, S., et al. 2021. The emerging role of ferroptosis in intestinal disease. *Cell Death & Disease* 12 (4): 289.
3. Huang, F., et al. 2022. STAT3-mediated ferroptosis is involved in ulcerative colitis. *Free Radical Biology & Medicine* 188: 375–385.
4. Salice, M., et al. 2019. A current overview of corticosteroid use in active ulcerative colitis. *Expert Review of Gastroenterology & Hepatology* 13 (6): 557–561.
5. Glover, L.E., J.S. Lee, and S.P. Colgan. 2016. Oxygen metabolism and barrier regulation in the intestinal mucosa. *The Journal of Clinical Investigation* 126 (10): 3680–3688.
6. Li, C., Y.Y. Cai, and Z.X. Yan. 2018. Brain-derived neurotrophic factor preserves intestinal mucosal barrier function and alters gut microbiota in mice. *Kaohsiung Journal of Medical Sciences* 34 (3): 134–141.

7. Ramanan, D., and K. Cadwell. 2016. Intrinsic defense mechanisms of the intestinal epithelium. *Cell Host & Microbe* 19 (4): 434–441.
8. Xu, D., et al. 2022. Orally administered ginkgolide C attenuates DSS-induced colitis by maintaining gut barrier integrity, inhibiting inflammatory responses, and regulating intestinal flora. *Journal of Agriculture and Food Chemistry* 70 (46): 14718–14731.
9. Lee, S.H. 2015. Intestinal permeability regulation by tight junction: Implication on inflammatory bowel diseases. *Intestinal Research* 13 (1): 11–18.
10. Chen, W.X., L.H. Ren, and R.H. Shi. 2014. Enteric microbiota leads to new therapeutic strategies for ulcerative colitis. *World Journal of Gastroenterology* 20 (42): 15657–15663.
11. Tan, A.H., S.Y. Lim, and A.E. Lang. 2022. The microbiome-gut-brain axis in Parkinson disease - from basic research to the clinic. *Nature Reviews Neurology* 18 (8): 476–495.
12. Xavier, R.J., and D.K. Podolsky. 2007. Unravelling the pathogenesis of inflammatory bowel disease. *Nature* 448 (7152): 427–434.
13. Schirmer, M., et al. 2019. Microbial genes and pathways in inflammatory bowel disease. *Nature Reviews Microbiology* 17 (8): 497–511.
14. Askari, V.R., et al. 2021. Anti-oxidant and anti-inflammatory effects of auraptene on phytohemagglutinin (PHA)-induced inflammation in human lymphocytes. *Pharmacological Reports* 73 (1): 154–162.
15. Genovese, S., and F. Epifano. 2011. Auraptene: A natural biologically active compound with multiple targets. *Current Drug Targets* 12 (3): 381–386.
16. Shao, X., et al. 2020. Anti-Inflammatory and Intestinal Microbiota Modulation Properties of Jinxiang Garlic (Allium sativum L.) Polysaccharides toward Dextran Sodium Sulfate-Induced Colitis. *Journal of Agricultural and Food Chemistry* 68 (44): 12295–12309.
17. Tayarani-Najaran, Z., N. Tayarani-Najaran, and S. Eghbali. 2021. A review of auraptene as an anticancer agent. *Frontiers in Pharmacology* 12: 698352.
18. Bibak, B., et al. 2019. A review of the pharmacological and therapeutic effects of auraptene. *BioFactors* 45 (6): 867–879.
19. Mizoguchi, A. 2012. Animal models of inflammatory bowel disease. *Progress in Molecular Biology and Translational Science* 105: 263–320.
20. Park, Y.H., et al. 2015. Adequate dextran sodium sulfate-induced colitis model in mice and effective outcome measurement method. *Journal of Cancer Prevention* 20 (4): 260–267.
21. Yang, L., et al. 2021. Tanshinone I and tanshinone IIA/B attenuate LPS-induced mastitis via regulating the NF-κB. *Biomedicine & Pharmacotherapy* 137: 111353.
22. Zhang, Y., et al. 2022. Alginate oligosaccharides ameliorate DSS-induced colitis through modulation of AMPK/NF-κB pathway and intestinal microbiota. *Nutrients* 14(14).
23. Zhao, Y., et al. 2018. GPR43 mediates microbiota metabolite SCFA regulation of antimicrobial peptide expression in intestinal epithelial cells via activation of mTOR and STAT3. *Mucosal Immunology* 11 (3): 752–762.
24. Yap, Y.A., and E. Marino. 2018. An insight into the intestinal web of mucosal immunity, microbiota, and diet in inflammation. *Frontiers in Immunology* 9: 2617.
25. Camilleri, M., et al. 2012. Intestinal barrier function in health and gastrointestinal disease. *Neurogastroenterology and Motility* 24 (6): 503–512.
26. Günzel, D., and M. Fromm. 2012. Claudins and other tight junction proteins. *Comprehensive Physiology* 2 (3): 1819–1852.
27. Cui, L., et al. 2021. Scutellaria baicalensis Georgi polysaccharide ameliorates DSS-induced ulcerative colitis by improving intestinal barrier function and modulating gut microbiota. *International Journal of Biological Macromolecules* 166: 1035–1045.
28. Akira, S., K. Takeda, and T. Kaisho. 2001. Toll-like receptors: Critical proteins linking innate and acquired immunity. *Nature Immunology* 2 (8): 675–680.
29. Vunta, H., et al. 2007. The anti-inflammatory effects of selenium are mediated through 15-deoxy-Delta 12,14-prostaglandin J2 in macrophages. *Journal of Biological Chemistry* 282 (25): 17964–17973.
30. Schottelius, A.J., and H. Dinter. 2006. Cytokines, NF-kappaB, microenvironment, intestinal inflammation and cancer. *Cancer Treatment and Research* 130: 67–87.
31. Shin, S.Y., et al. 2016. The UPR inducer DPP23 inhibits the metastatic potential of MDA-MB-231 human breast cancer cells by targeting the Akt-IKK-NF-κB-MMP-9 axis. *Science and Reports* 6: 34134.
32. Stojanov, S., A. Berlec, and B. Strukelj. 2020. The influence of probiotics on the firmicutes/bacteroidetes ratio in the treatment of obesity and inflammatory bowel disease. *Microorganisms* 8(11).
33. Dias, A.M.M., et al. 2021. Lactobacillus stress protein GroEL prevents colonic inflammation. *Journal of Gastroenterology* 56 (5): 442–455.
34. Vallianou, N., et al. 2021. Do antibiotics cause obesity through long-term alterations in the gut microbiome? A review of current evidence. *Current Obesity Reports* 10 (3): 244–262.